

# Chemosensitive Conductance and Inositol 1,4,5-Trisphosphate-induced Conductance in Snake Vomeronasal Receptor Neurons

Mutsuo Taniguchi, Dalton Wang<sup>1</sup> and Mimi Halpern

Departments of Anatomy and Cell Biology and <sup>1</sup>Biochemistry, State University of New York Health Science Center at Brooklyn, 450 Clarkson Avenue, NY 11203, USA

Correspondence to be sent to: Dr Mimi Halpern, Department of Anatomy and Cell Biology, SUNY Health Science Center at Brooklyn, 450 Clarkson Avenue, Box 5, Brooklyn, NY 11203, USA. e-mail: mhalpern@netmail.hscbklyn.edu

## Abstract

Snake vomeronasal receptor neurons in slice preparations were studied using the patch-clamp technique in the conventional and nystatin-perforated whole-cell configurations. The mean resting potential was approximately  $-70$  mV; the average input resistance was  $3$  G $\Omega$ . Neurons required current injection of only  $1$ – $10$  pA to display a variety of spiking patterns. Intracellular dialysis of  $100$   $\mu$ M inositol 1,4,5-trisphosphate (IP<sub>3</sub>) evoked an inward current in 38% of neurons, with an average peak amplitude of  $16.4 \pm 2.8$  pA at a holding potential of  $-70$  mV. Application of  $100$   $\mu$ M 3-deoxy-3-fluoro-D-*myo*-inositol 1,4,5-trisphosphate (F-IP<sub>3</sub>), a derivative of IP<sub>3</sub>, also evoked an inward current in 4/8 (50%) neurons ( $32.6 \pm 58$  pA at  $-70$  mV,  $n = 4$ ). The reversal potentials of the induced components were estimated to be  $-14 \pm 5$  mV for IP<sub>3</sub> and  $-17 \pm 3$  mV for F-IP<sub>3</sub>. Bathing the neurons in  $10$   $\mu$ M ruthenium red solution greatly reduced the IP<sub>3</sub>-evoked inward current to  $1.6 \pm 1.1$  pA at  $-70$  mV ( $n = 6$ ). With Cs<sup>+</sup>-containing internal solution, neither the Ca<sup>2+</sup>-ATPase inhibitor thapsigargin ( $1$ – $50$   $\mu$ M) nor the Ca<sup>2+</sup>-ionophore ionomycin ( $10$   $\mu$ M) evoked a significant current response, suggesting that IP<sub>3</sub> can elicit current response in the neurons without mediation by intracellular Ca<sup>2+</sup> stores. Intracellular application of  $1$  mM cAMP evoked no detectable current response. Extracellular application of chemoattractant for snakes evoked a very large inward current. The reversal potential of the chemoattractant-induced current was similar to that of the IP<sub>3</sub>-induced current. The present results suggest that IP<sub>3</sub> may act as a second messenger in the transduction of chemoattractants in the garter snake vomeronasal organ.

## Introduction

The vomeronasal (VN) system is a nasal chemosensory system distinguished from the main olfactory system in most terrestrial vertebrates. In snakes, where the vomeronasal organ (VNO) is particularly well developed and has taken the role as the principal olfactory organ, it mediates prey detection, feeding and reproduction (Halpern, 1987). One of the best characterized stimuli for the garter snake VNO is a 20 kDa glycoprotein derived from earthworm shock secretion (Jiang *et al.*, 1990). This chemoattractant has been purified to homogeneity (Jiang *et al.*, 1990) and its gene sequence cloned (Liu *et al.*, 1997). Binding of this ligand to its G-protein-coupled receptors on VN bipolar neurons leads to an increase in intracellular inositol 1,4,5-trisphosphate (IP<sub>3</sub>) accumulation, a decrease in basal levels of cAMP (Luo *et al.*, 1994) and increased firing of mitral cells in the accessory olfactory bulb (Jiang *et al.*, 1990). These results suggest that chemosignal transduction in snake VN receptor neurons is mediated by these second messenger pathways.

Chemosignal transduction in the VNO can be elucidated by observing the physiological effects of its ligand and/or the action of components of second-messenger systems

such as the IP<sub>3</sub> or cAMP cascades. Although several approaches have been used to examine the effects of putative second-messenger molecules on the membrane conductance of VN sensory neurons using the patch-clamp technique (Trotier *et al.*, 1994; Taniguchi *et al.*, 1995, 1996; Liman and Corey, 1996; Inamura *et al.*, 1997a), IP<sub>3</sub>-mediated conductance in VN receptor neurons were found only in turtle and rat (Taniguchi *et al.*, 1995; Inamura *et al.*, 1997a). However, very few responses to physiologically relevant stimuli have been determined (Moss *et al.*, 1997).

To investigate the role of second messengers in VN signal transduction in snakes, IP<sub>3</sub> and its derivative were dialyzed into snake VN neurons in slice preparations using the patch-clamp technique in the whole-cell configuration, and the evoked current was measured. In addition, we characterized the response to physiologically relevant stimuli, the chemoattractants found in electric shock-induced earthworm secretion. We found that dialysis of IP<sub>3</sub> into VN neurons elicited an inward current, the reversal potential of which was similar to that of the response induced by the earthworm-derived chemoattractants. These findings provide evidence of IP<sub>3</sub>-activated conductance in the membrane of

VN receptor neurons. Although the voltage-gated currents underlying the excitatory response form an essential part of the VN transduction process, no prior patch-clamp study has been conducted in the snake VNO. Thus, we also examined some electrophysiological features of snake VN receptor neurons.

## Materials and methods

### Slice preparation of VN epithelium

Garter snakes, *Thamnophis sirtalis*, weighing 34–131 g, were obtained from commercial suppliers and maintained at 22°C. The methods were essentially similar to those described previously (Taniguchi *et al.* 1996). In brief, VN neuroepithelia were dissected out from decapitated snakes and cut into slices ~120 µm thick with a vibrating slicer (Vibratome 3000, Technical Products International Inc., St Louis, MO) in Ringer's solution. An epithelial slice was then fixed on the glass surface of a recording chamber. This permitted access to cells on the surface of the slice by the patch pipette. The preparations were viewed under an upright microscope (Optiphot UD-2, Nikon, Tokyo, Japan) using a ×40 water immersion lens (Zeiss).

### Data recording and analysis

Membrane currents were recorded in the conventional or perforated whole-cell configuration (holding potential, -70 mV). All results were obtained under conventional whole-cell configuration (Hamill *et al.*, 1981) except in the case where a response to chemoattractants was recorded. For conventional and perforated whole-cell configuration, patch pipettes with resistances of 5–10 and 3–5 MΩ, respectively, were made from borosilicate glass capillaries (A-M Systems, Inc., Everett, WA) using a two-stage electrode puller (model PP83, Narishige, Tokyo, Japan) and then heat-polished. Measurements were made using a Dagan patch-clamp amplifier (model 8900, Dagan Co., Minneapolis, MN). Data were stored on videocassette using an instrumentation recorder (model 420-B, A.R. Vetter Co., Rebersburg, PA) or an IBM-PC compatible personal computer. Data were sampled at least three times the filtering frequency (30–10 kHz) and digitized with the Digidata 1200 interface (Axon Instruments, Inc., Foster City, CA). Analysis was performed on a personal computer using pCLAMP software (Axon Instruments, Inc.). The membrane conductances were derived from least-squares regression of the membrane current amplitude recorded at membrane potentials ranging from -100 to +100 mV. All recordings were performed at room temperature. All values are given as mean ± SEM. Significance of differences between means was assessed using the Student's *t*-test.

### Lucifer yellow dialysis

In the experiments using conventional whole-cell configuration, tips of the patch pipettes containing a glass

filament were filled with an internal solution containing 0.2% Lucifer yellow CH. After experiments in this configuration were complete, the pipettes were pulled back from the surface of the tested cells so that the membranes resealed. The specimens were then viewed with fluorescent illumination.

### Solutions

Normal Ringer's solution consisted of (in mM): 119 NaCl, 4.1 KCl, 2.5 CaCl<sub>2</sub>, 1.5 MgCl<sub>2</sub>, 15 glucose, 5 Na-pyruvate, 10 HEPES-NaOH, pH 7.4. Patch pipettes were filled with a normal internal solution (K<sup>+</sup>-internal; in mM): 132.1 KCl, 0.1 CaCl<sub>2</sub>, 3.6 MgCl<sub>2</sub>, 1 EGTA, 2.5 Na<sub>2</sub>ATP, 0.2% Lucifer yellow CH, 10 HEPES-KOH, pH 7.6. In some experiments KCl was replaced with CsCl (Cs<sup>+</sup>-internal) and the pH was adjusted with CsOH. cAMP, IP<sub>3</sub> and 3-deoxy-3-fluoro-D-*myo*-inositol 1,4,5-trisphosphate (F-IP<sub>3</sub>) were dissolved in the Cs<sup>+</sup>-internal solution to desired final concentrations. Thapsigargin, ionomycin or ruthenium red was dissolved in Ringer's solution. For perforated whole-cell recording, nystatin was dissolved in normal internal solution containing (in mM) 5 *N*-methyl-D-glucamine, 5 methanesulfonic acid, 0.5 phenol red at a final concentration of 250 mg/ml. No Lucifer yellow CH was included in the pipette solution for perforated whole-cell recording. Electric shock-induced earthworm secretion prepared as described elsewhere (Jiang *et al.*, 1990), which includes chemoattractants, was diluted with Ringer's solution.

Gravity was used to deliver a constant stream of Ringer's solution from the stimulating tube. Two electrically actuated valves were used to switch irrigating Ringer's solution and a stimulating solution. The stimulating tube with a lumen 160–200 µm in diameter was placed under visual control within ~500 µm of the neuron. To eliminate a nonspecific effect of mechanical stimulation, a slice was irrigated with Ringer's solution at the same flow rate as that of the stimulating solution prior to application of the stimulating solution. The concentrations of stimuli are represented as concentration in the pipette, and no correction for dilution has been made.

### Histological observations

For histological examination of sections of the VN epithelium (Figure 1A), animals were anesthetized with Metofane (Pitman-Moore, Inc., Mundelein, IL) and perfused intracardially with saline, followed by Bodian's fixative (Bodian, 1936). The heads were stored in fixative for several days and decalcified for 2–3 days in DECAL (Omega Chemical Corp., Cold Spring, NY) containing 9.5% HCl and catalytic calcium ion chelating agent, followed by a wash in running tap water for 3 h. Tissues were dehydrated and embedded in paraplast (Oxford Labware, St Louis, MO). Twelve-micrometer paraffin sections were cut in the horizontal plane. The mounted sections were impregnated with 1% Protargol S (without copper) for 18–24 h at room

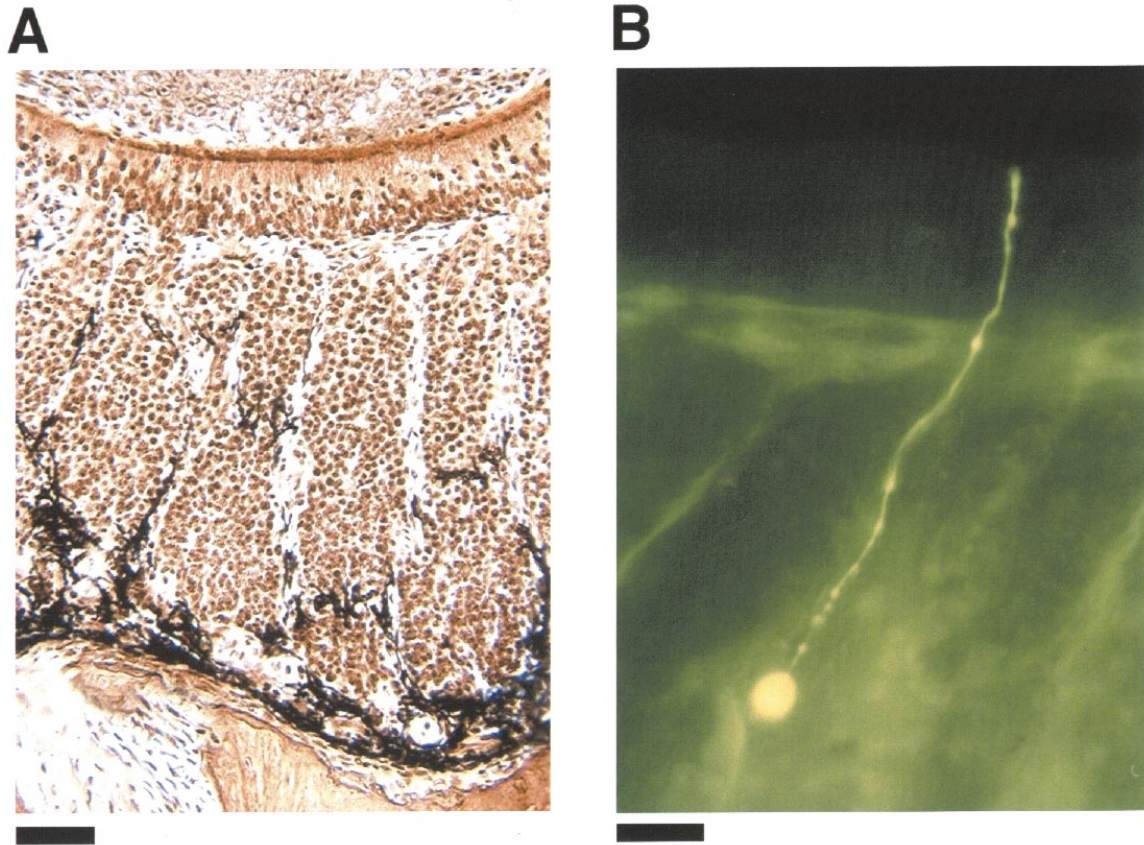


**Figure 1** Snake VN sensory epithelium. **(A)** Photomicrograph of a slice of VN epithelium. Bar = 50  $\mu$ m. **(B)** Fluorescence micrograph of a receptor neuron in the sensory epithelium. The neuron was dialyzed with 0.2% Lucifer yellow. The cell body and dendrite, which projects to the epithelial surface, are visible. Bar = 25  $\mu$ m.

temperature. Tissues on the slide were reduced and fixed according to the method reported by Bodian (1936, 1937).

### Chemicals

IP<sub>3</sub>, F-IP<sub>3</sub>, ionomycin and thapsigargin were purchased from Calbiochem-Novabiochem Corp. (La Jolla, CA). cAMP, Lucifer yellow CH and ruthenium red were purchased from Sigma (St Louis, MO). All other reagents were the highest grade commercially available.

## Results

### Cell morphology

The sensory epithelium of garter snakes consists of a supporting cell layer, a receptor cell layer and an undifferentiated cell layer (Wang and Halpern, 1980). A highly segregated lamination exists in which supporting cells are separated from the deeper layers (Figure 1A). Though the receptor and basal cell layers are morphologically indistinguishable from each other with an optical microscope, the apically situated receptor cell layer is quite deep (~20–30 cells thick) and the basally situated undifferentiated cell

layer is relatively thin (4–6 cells deep) (Wang and Halpern, 1980).

Vomeronasal receptor cells are bipolar neurons whose dendrites terminate as microvilli at the luminal surface of the VNO (Wang and Halpern, 1980). The microvilli themselves could not be visualized with the optics used for these electrophysiological experiments due to their small diameter, 100 nm (Wang and Halpern, 1980). Cells in the estimated bipolar cell layer dialyzed with 0.2% Lucifer yellow had a morphology characteristic of VN receptor neurons (Figure 1B). Dendrites of these dialyzed cells were clearly visualized projecting to the epithelial surface.

Vomeronasal receptor neurons were identified by their ability to respond to voltage stimulation and their typical morphology. Thus, we monitored the morphology of each cell in which we made recordings in whole-cell configuration. All data were taken from neurons that showed response to depolarizing voltage steps from a holding potential (see below) and had identifiable dendrites.

### Voltage responses to injected current

With normal internal solution in the pipette, snake VN receptor neurons maintained resting potentials ranging

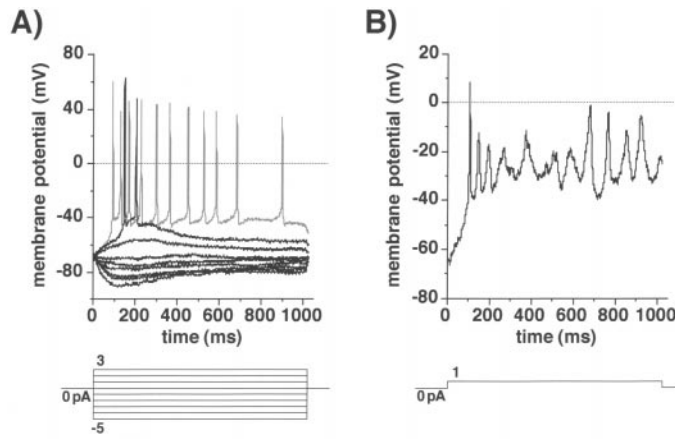


**Figure 2** Current-clamp recordings from snake VN receptor neurons. **(A)** Voltage response of a VN neuron to injected current steps between  $-5$  and  $+3$  pA in  $1$  pA increments. In this case, the action potentials were generated repetitively when a depolarizing current pulse of  $2$  pA was injected. The resting level of this neuron was  $-69$  mV and threshold was near  $-50$  mV. **(B)** Voltage response of another VN receptor neuron to a current step of  $1$  pA. Bottom traces show the corresponding current pulse. In both cases, the patch pipette contained normal internal solution.

from  $-63$  to  $-85$  mV ( $-73 \pm 2$  mV;  $n = 16$ ). The input resistance, measured by injection of current pulses of a few pA, ranged from  $1.1$  to  $6.1$  G $\Omega$  ( $3.4 \pm 0.4$  G $\Omega$ ;  $n = 16$ ).

In current-clamp recordings, step depolarization induced by stimulus current produced action potentials (Figure 2). The threshold for action potential generation in VN receptor neurons was commonly between  $-38$  and  $-58$  mV, with a mean threshold potential of  $-50 \pm 1$  ( $n = 16$ ). A variety of spiking patterns was seen, ranging from neurons that fired only a single action potential for any supra-threshold stimulus examined (data not shown) to those that generated brief trains of action potentials. In most of the neurons which fired repetitively in response to injected current, the firing frequency increased with increasing current and an oscillatory pattern appeared when the magnitude of the injected current was increased further (data not shown). The current amplitude at which the membrane settled into oscillations differed among the neurons and ranged from  $3$  to  $20$  pA. Because of this large variation among the neurons, we did not perform a quantitative analysis of the relationship between magnitude of injected current and firing frequency. The maximal firing frequency was  $25$  impulses/s. In the example shown in Figure 2A, the action potentials were generated repetitively in response to a depolarizing current pulse of  $2$  or  $3$  pA with no sign of adaptation during a  $1$  s step. In  $6/16$  neurons, an injected current of  $1$  pA was enough to elicit action potential(s) (e.g. see Figure 2B).

Action potentials were evoked by a small current of only  $1$ – $10$  pA injected into snake VN receptor neurons, suggesting that sensitivity of these neurons to current stimulation

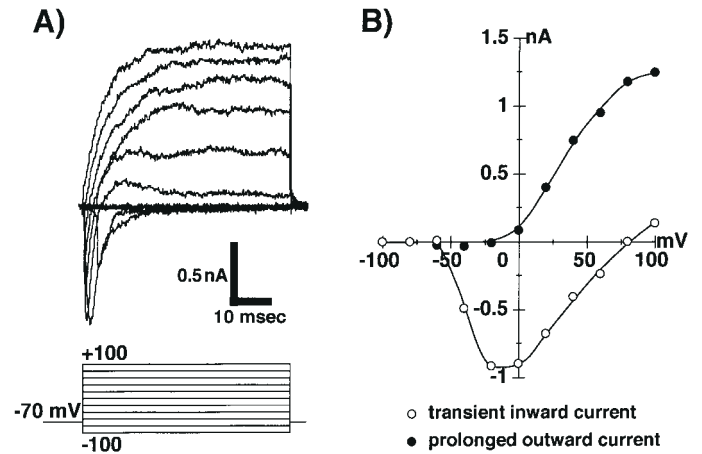


**Figure 3** Typical whole-cell currents in a VN receptor neuron in a slice preparation. **(A)** Response to voltage steps. Step levels are shown in the bottom traces. Transient inward and delayed outward currents were elicited in response to  $60$  ms voltage steps between  $-100$  and  $+100$  mV in  $20$  mV increments from a holding potential of  $-70$  mV. **(B)** Current–voltage relationships of peak inward currents ( $\circ$ ) and  $60$  ms after the onset of the voltage step during the sustained plateau of the outward current ( $\bullet$ ) measured from the records in A. The pipette contained normal internal solution ( $K^+$ -internal) and the bath contained Ringer's solution.

is similar to that reported for frog, turtle, mouse and rat (Trotier *et al.*, 1993; Liman and Corey, 1996; Taniguchi *et al.*, 1996; Inamura *et al.*, 1997a).

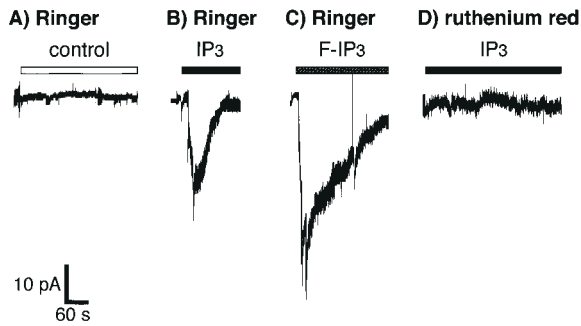
#### Whole-cell currents

Figure 3A illustrates the two major currents elicited by depolarizing steps of voltage from a holding potential of  $-70$  mV. A transient inward current activated at  $-40$  mV increased as the depolarizing steps approached  $-20$  mV. The transient inward current was maximal, near  $1$  nA, at  $-20$  mV. With further depolarization, this rapid inward current diminished but the subsequent outward current continued to increase as a function of the step voltage (Figure 3B).

The outward currents were blocked when  $Cs^+$  was substituted for  $K^+$  in the internal pipette solution (data not shown), indicating that the outward current was mainly carried by  $K^+$  ions. These measurements are in general agreement with those previously reported in VN neurons of other species (Trotier *et al.*, 1993, 1994; Liman and Corey, 1996; Taniguchi *et al.*, 1996; Inamura *et al.*, 1997a).

#### Current induced by $IP_3$ and its derivative

To confirm the existence of  $IP_3$ -mediated conductance in snake VN receptor neurons,  $IP_3$  was introduced into a part of the cell soma using conventional whole-cell configuration. Figure 4 shows the currents induced by intracellular dialysis of  $IP_3$  and F- $IP_3$ , a derivative of  $IP_3$  which cannot be metabolized to  $IP_4$ . When the pipette was filled with an  $IP_3$ -free internal solution, a steady baseline was recorded at



**Figure 4** Response induced by intracellular application of IP<sub>3</sub> and its derivative. **(A)** Response induced by intracellular application of 0 μM IP<sub>3</sub> into a VN neuron bathed in normal Ringer's solution. **(B)** Response induced by intracellular application of 100 μM IP<sub>3</sub> into a VN neuron bathed in normal Ringer's solution. **(C)** Response induced by intracellular application of 100 μM F-IP<sub>3</sub>, a derivative of IP<sub>3</sub> which cannot be metabolized to IP<sub>4</sub>, into a VN neuron bathed in normal Ringer's solution. **(D)** Response induced by intracellular application of 100 μM IP<sub>3</sub> into a VN neuron bathed in Ringer's solution containing 10 μM ruthenium red. The patch pipette contained Cs<sup>+</sup>-internal solution with or without IP<sub>3</sub> compounds. Holding potential, -70 mV.

a holding potential of -70 mV over the test interval of 5–10 min after membrane rupture (Figure 4A). On the other hand, intracellular application of 100 μM IP<sub>3</sub> evoked an inward current in 6/16 neurons (38%), with adaptation of current after the peak response (Figure 4B). The mean amplitude of the inward current induced by IP<sub>3</sub> was  $16.4 \pm 2.8$  pA ( $n = 6$ ). The time-to-peak for the response of the VN neurons varied from 12 to 27 s ( $22 \pm 2$  s;  $n = 6$ ). This time course was similar to that for IP<sub>3</sub>-induced response of turtle VN neurons (Taniguchi *et al.*, 1995) but was much faster than that of rat olfactory neurons (30–1200 s) (Okada *et al.*, 1994).

In the VN neurons of turtle (Taniguchi *et al.*, 1995) and rat (Inamura *et al.*, 1997a), the IP<sub>3</sub>-induced response was inhibited by 10 μM ruthenium red. We examined the effect of ruthenium red on IP<sub>3</sub>-induced response in snake VN neurons (Figure 4D). Bathing the neurons in 10 μM ruthenium red solution greatly reduced IP<sub>3</sub>-induced inward currents. The mean peak amplitude of the IP<sub>3</sub>-induced current in the presence of ruthenium red was  $1.6 \pm 1.1$  pA ( $n = 6$ ).

Intracellular dialysis of F-IP<sub>3</sub>, the non-metabolizable analogue of IP<sub>3</sub>, also elicited an inward current in 4/8 neurons (50%) with an average peak amplitude of  $32 \pm 5.8$  pA ( $n = 4$ ; Figure 4C). Though F-IP<sub>3</sub> is not converted to IP<sub>4</sub>, the response induced by F-IP<sub>3</sub> also displayed adaptation, suggesting that this adaptation may be due to desensitization of the IP<sub>3</sub> channel in the receptor membrane. The mean time-to-peak for the response of the VN neurons to F-IP<sub>3</sub> was  $24 \pm 7$  s, range 4–31 s ( $n = 4$ ). These values are not statistically different from those for the response induced by IP<sub>3</sub>.

In mammals, immunohistochemical and molecular bio-

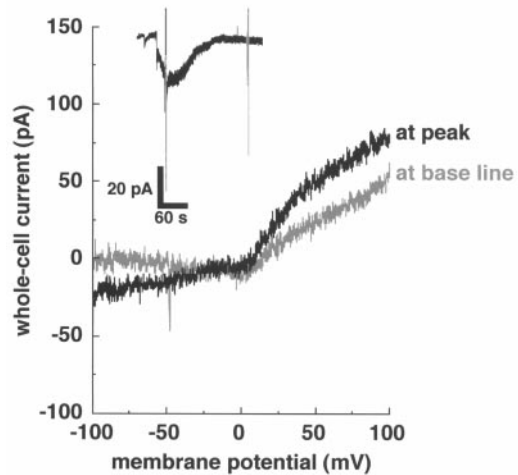


**Figure 5** Whole-cell  $I$ - $V$  relationships for the current evoked by intracellular application of 100 μM IP<sub>3</sub>. The whole-cell current was measured by applying a voltage ramp (65.9 mV/s) from -100 to +100 mV during and after the response induced by 100 μM IP<sub>3</sub>. These traces were obtained from the same cell. The inset shows the record of the IP<sub>3</sub>-induced response of this neuron under whole-cell voltage-clamp conditions at -70 mV. The current transients were produced by the voltage-ramps. The pipette contained Cs<sup>+</sup>-internal solution. The reversal potential of the current induced by intracellular application of IP<sub>3</sub> to this neuron was estimated to be -16 mV.

logical studies have demonstrated the spatially segregated subsets of VN receptor neurons that form longitudinal zones in the VN neuroepithelium (Dulac and Axel, 1995; Halpern *et al.*, 1995; Berghard and Buck, 1996; Jia and Halpern, 1996; Herrada and Dulac, 1997; Matsunami and Buck, 1997; Ryba and Tirindelli, 1997). However, no such segregation has been reported in the garter snake VN epithelium (Luo *et al.*, 1994). If such a segregation exists in the snake VNO but previously had been undetected, one might expect to see differences in response to injections of IP<sub>3</sub> at different levels of the epithelium. To examine whether neurons with somas at different locations in the epithelium responded to IP<sub>3</sub> differently, the relative location of a soma of the IP<sub>3</sub>-injected neurons in the neuroepithelium was measured. The basal–apical axis of the neuron layer in the epithelium was defined as 0 (basal) and 100 (apical), i.e. the closer the value was to 100, the more apically situated was the soma of the neuron in the receptor cell layer. The mean relative location of the neurons that responded or did not respond to IP<sub>3</sub> was  $39.5 \pm 7.2$  ( $n = 6$ ) and  $48.0 \pm 3.6$  ( $n = 10$ ) respectively. In the same way, the mean relative location of the neurons that responded and did not respond to F-IP<sub>3</sub> was  $53.3 \pm 6.3$  ( $n = 4$ ) and  $48.5 \pm 9.9$  ( $n = 4$ ) respectively. Thus, there was no significant regional difference between the neurons that responded and those that did not respond to IP<sub>3</sub> or F-IP<sub>3</sub>.

#### Voltage dependence of IP<sub>3</sub>-induced response

The current–voltage ( $I$ - $V$ ) relationships of the IP<sub>3</sub>-induced response were examined by applying a voltage ramp from

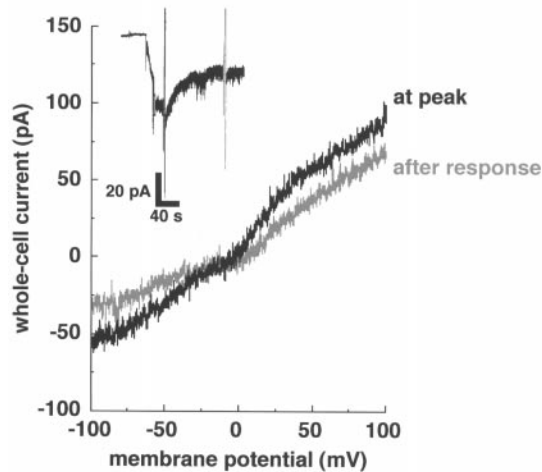


**Figure 6** Whole-cell  $I$ - $V$  relationships for the current evoked by intracellular application of  $100 \mu\text{M}$  F- $\text{IP}_3$ . The whole-cell current was measured by applying a voltage ramp ( $65.9 \text{ mV/s}$ ) from  $-100$  to  $+100 \text{ mV}$  during and after the response induced by  $100 \mu\text{M}$  F- $\text{IP}_3$ . These traces were obtained from the same cell. The inset shows the record of the F- $\text{IP}_3$ -induced response of this neuron under whole-cell voltage-clamp conditions at  $-70 \text{ mV}$ . The current transients were produced by the voltage-ramps. The patch pipette contained  $\text{Cs}^+$ -internal solution. The reversal potential of the current induced by intracellular application of F- $\text{IP}_3$  to this neuron was estimated to be  $-11 \text{ mV}$ .

$-100$  to  $+100 \text{ mV}$  ( $65.9 \text{ mV/s}$ ) to voltage-clamped VN neurons near the peak of the response, and after the response induced by  $\text{IP}_3$  (Figure 5). As shown in Figure 5, the slope of the  $I$ - $V$  curve measured near the peak of the response was steeper than that measured after the response. The membrane conductances were  $393 \pm 41 \text{ pS}$  ( $n = 6$ ) and  $224 \pm 19 \text{ pS}$  ( $n = 6$ ) during and after the responses, respectively. These values were significantly different ( $P < 0.01$ ), indicating that  $\text{IP}_3$  increases the membrane conductance. The mean reversal potential was estimated to be  $-14 \pm 5 \text{ mV}$  ( $n = 6$ ).

Figure 6 shows the voltage-dependence of inward currents induced by  $100 \mu\text{M}$  F- $\text{IP}_3$ . The slope of the  $I$ - $V$  curve measured during the F- $\text{IP}_3$ -induced response was steeper than that measured after the response. The membrane conductances were  $819 \pm 108$  ( $n = 4$ ) and  $496 \pm 66 \text{ pS}$  ( $n = 4$ ) during and after the responses respectively. These values were significantly different ( $P < 0.07$ ), suggesting that F- $\text{IP}_3$  increases membrane conductance. The reversal potential was estimated to be  $-17 \pm 3 \text{ mV}$  ( $n = 4$ ) and was not statistically different from that observed in response to intracellular application of  $\text{IP}_3$  as shown in Figure 5.

The membrane conductance measured with both applications of  $\text{IP}_3$  dissolved in the  $\text{Cs}^+$ -internal solutions and  $10 \mu\text{M}$  ruthenium red in the bath was  $403 \pm 26 \text{ nS}$  ( $n = 6$ ). This value is smaller than that measured during the F- $\text{IP}_3$ -induced response ( $P < 0.005$ ), but is larger than that measured without ruthenium red in the bath nor  $\text{IP}_3$  in the

pipette ( $258 \pm 22 \text{ nS}$ ,  $n = 18$ ,  $P < 0.005$ ). These results suggest that ruthenium red has a side effect of increasing membrane conductance. Increased membrane conductance by external application of ruthenium red was reported in rat olfactory neurons (Okada *et al.*, 1994).

#### Effect of ionomycin and thapsigargin on whole-cell currents

It is well established that  $\text{IP}_3$  induces release of  $\text{Ca}^{2+}$  from internal stores in response to hormones and neurotransmitters (Ferris and Snyder 1992; Berridge 1993). Thus there is a possibility that the responses of snake VN receptor neurons to  $\text{IP}_3$  are mediated by  $\text{IP}_3$ -induced increases in cytosolic  $\text{Ca}^{2+}$ . To examine this possibility, we investigated the effect of increases in intracellular  $\text{Ca}^{2+}$  elicited by addition of the  $\text{Ca}^{2+}$ -ionophore ionomycin on whole-cell currents in snake VN neurons. When the neurons were dialyzed with normal internal solution ( $\text{K}^+$ -internal), extracellular application of  $10 \mu\text{M}$  ionomycin evoked a prolonged outward current with an average peak amplitude of  $24.5 \pm 8.2 \text{ pA}$  in 5/5 neurons (Figure 7A). The mean resting potential decreased slightly from  $-78 \pm 11$  ( $n = 5$ ) to  $-80 \pm 4$  ( $n = 5$ ). Figure 7C shows the voltage-dependence of outward currents induced by  $10 \mu\text{M}$  ionomycin. At negative membrane potentials less than  $-20 \text{ mV}$ , the slope of the  $I$ - $V$  curve measured during the response to ionomycin is steeper than that measured before the response. The reversal potential was estimated to be  $-82 \pm 2 \text{ mV}$  ( $n = 5$ ). The reversal potential of ionomycin-induced current was near the estimated equilibrium potential of  $\text{K}^+$  in the present condition ( $-88 \text{ mV}$  at  $20^\circ\text{C}$ ) but was different from that of the  $\text{IP}_3$ -induced current ( $P < 0.0001$ ). Replacement of  $\text{K}^+$  with  $\text{Cs}^+$  in the internal solution completely blocked the ionomycin-induced outward current in 6/6 neurons (Figure 7B). The membrane conductance before an application of ionomycin with  $\text{Cs}^+$ -internal solution ( $217 \pm 28 \text{ nS}$ ;  $n = 5$ ) was similar to that during application of ionomycin ( $212 \pm 24 \text{ nS}$ ;  $n = 5$ ). These results suggest that  $\text{Ca}^{2+}$ -activated  $\text{K}^+$  current is the major component of the ionomycin-induced current.

We also investigated the effect on snake VN receptor neurons of the  $\text{Ca}^{2+}$ -ATPase inhibitor thapsigargin. When the neurons were dialyzed with normal internal solution ( $\text{K}^+$ -internal), extracellular application of  $10 \mu\text{M}$  thapsigargin evoked a prolonged outward current in 3/4 neurons (data not shown). In preparations in which  $\text{Cs}^+$  replaced  $\text{K}^+$  in the pipette, extracellular application of thapsigargin at concentrations of 1, 10 or  $50 \mu\text{M}$  evoked no significant current response ( $n = 5$  for each concentration of thapsigargin, data not shown). The results shown in Figure 7 and described here suggest that  $\text{IP}_3$  can elicit an inward current without mediation by intracellular  $\text{Ca}^{2+}$  stores.

#### Current response to cAMP

Biochemical studies have demonstrated that functional

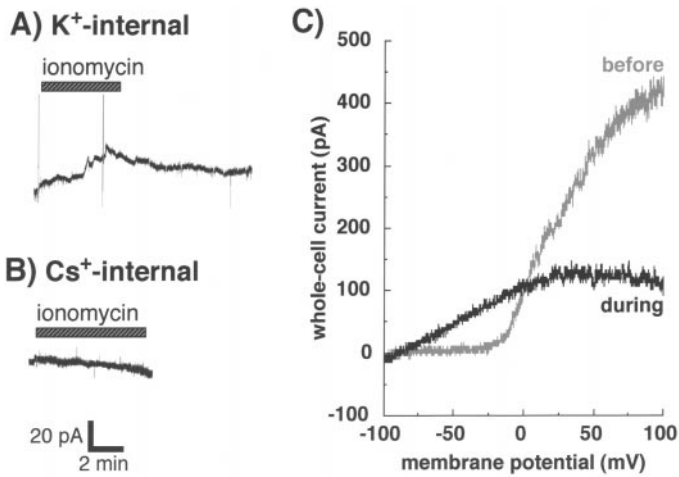


**Figure 7** Effect of increases in intracellular  $\text{Ca}^{2+}$ , evoked by extracellular application of the  $\text{Ca}^{2+}$ -ionophore ionomycin, on whole-cell currents. **(A)** Response induced by extracellular application of  $10 \mu\text{M}$  ionomycin to a VN neuron under whole-cell voltage-clamp conditions. The current transients were produced by the voltage-ramps (see C). The patch pipette contained normal internal solution ( $\text{K}^+$ -internal). **(B)** Response induced by extracellular application of  $10 \mu\text{M}$  ionomycin to a VN neuron when the patch pipette contained  $\text{Cs}^+$ -internal solution. Outward current induced by ionomycin was blocked by replacement of  $\text{K}^+$  in the pipette solution with  $\text{Cs}^+$ . Holding potential,  $-70 \text{ mV}$ . **(C)** Whole-cell  $I-V$  relationships for the current evoked by extracellular application of  $10 \mu\text{M}$  ionomycin to a VN neuron shown in A. The whole-cell current was measured by applying a voltage ramp ( $65.9 \text{ mV/s}$ ) from  $-100$  to  $+100 \text{ mV}$  before and during the response induced by  $10 \mu\text{M}$  ionomycin to a VN neuron shown in A. These traces were obtained from the same cell. The patch pipette contained normal internal solution ( $\text{K}^+$ -internal). The reversal potential at negative membrane potentials of the current induced by extracellular application of ionomycin to this neuron was estimated to be  $-89 \text{ mV}$ .

adenylyl cyclase exists in snake and turtle VN sensory epithelia; application of forskolin, guanosine triphosphate (GTP) and guanosine 5'-3-*O*-(thio)triphosphate ( $\text{GTP}\gamma\text{S}$ ) to membrane preparations of the snake and the turtle VN epithelia induced cAMP accumulation (Luo *et al.*, 1994; Okamoto *et al.*, 1996). In 10 neurons, however, we detected no response to  $1 \text{ mM}$  cAMP (Figure 8).

#### Current response to chemoattractants and its voltage dependence

Repeated attempts to obtain current responses to the chemoattractants in earthworm electric shock secretion (ESS) in the conventional whole-cell configuration were unsuccessful, even in cells that exhibited normal responses to injected currents or depolarizations with voltage steps ( $n = 7$ ). However, we were successful in obtaining such responses to ESS in the perforated whole-cell configuration (Figure 9A). Application of the chemoattractants in ESS ( $\sim 12 \text{ mg/ml}$  protein) to the apical portion of the neurons evoked an inward current in  $3/4$  neurons, with an average peak amplitude of  $791 \pm 217 \text{ pA}$  ( $n = 3$ ).

Figure 9B illustrates the voltage dependence of the

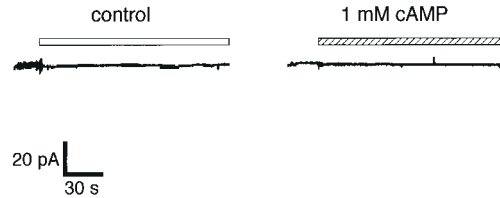


**Figure 8** Response induced by intracellular application of  $0 \mu\text{M}$  cAMP (left trace) and  $1 \text{ mM}$  cAMP (right trace). The patch pipette contained  $\text{Cs}^+$ -internal solution with or without cAMP. Bars above traces indicate period of intracellular dialysis of  $0$  and  $1 \text{ mM}$  cAMP. Holding potential,  $-70 \text{ mV}$ .

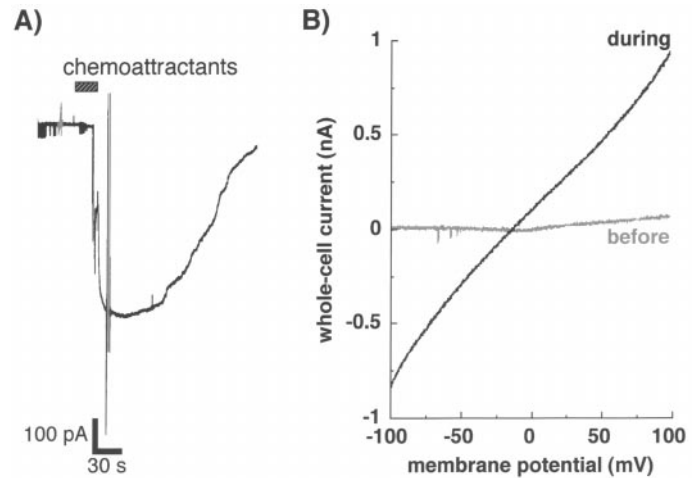


**Figure 9** **(A)** Response of a VN receptor neuron to chemoattractants ( $13.2 \text{ mg/ml}$  protein) applied to its surface under perforated whole-cell configuration in voltage-clamp mode at  $-70 \text{ mV}$ . The current transients were produced by the voltage-ramps. The patch pipette contained  $\text{Cs}^+$ -internal solution. Hatched bar above the trace indicates period of application of chemoattractants. **(B)** The whole-cell  $I-V$  relationships for the current evoked by extracellular application of chemoattractants. The current was measured by applying a voltage ramp ( $65.9 \text{ mV/s}$ ) from  $-100$  to  $+100 \text{ mV}$  before and during the response induced by application of chemoattractants to a VN neuron shown in A. These traces were obtained from the same cell. The reversal potential of the chemoattractants-induced current to this neuron was estimated to be  $-12 \text{ mV}$ .

chemoattractants-induced currents examined by applying a voltage ramp from  $-100$  to  $+100 \text{ mV}$  ( $65.9 \text{ mV/s}$ ) to voltage-clamped neurons before and during the response induced by chemoattractants. The slope of the  $I-V$  curve measured during the response to chemoattractants was steeper than that measured before the application of chemoattractants. The membrane conductances were  $331 \pm 49$  ( $n = 3$ ) and  $7557 \pm 2093 \text{ pS}$  ( $n = 3$ ) during and after the responses respectively. These values were significantly different ( $P < 0.05$ ), indicating that response to chemoattractants was evoked by an increase in membrane conductance. The mean reversal potential of the chemoattractants-induced current was estimated to be  $-21 \pm 5 \text{ mV}$  ( $n = 3$ ) and was similar to that observed in response to intracellular application of  $\text{IP}_3$  or  $\text{F-IP}_3$ , as shown in Figures 5 and 6.

## Discussion

### Electrophysiological features of snake VN receptor neurons

Snake VN receptor neurons have a mean resting potential of  $-73$  mV, somewhat more negative than those of VN receptor neurons in turtles (Taniguchi *et al.*, 1996), mice (Liman and Corey, 1996) and rats (Inamura *et al.*, 1997a), which were reported to be  $-48$ ,  $-58$  and  $-46$  mV, respectively. On the other hand, the mean resting potential is less negative than that in frogs which was reported to be  $-88$  mV (Trotier and Døving, 1996a). Input resistance of the snake neurons at rest was  $3.4$  G $\Omega$ . As a result of the high input resistance of the snake VN receptor neurons, an injected current as small as  $1$  pA reached spike threshold in some neurons. This is similar to the case for VN neurons of other vertebrates (Trotier *et al.*, 1993; Liman and Corey, 1996; Taniguchi *et al.*, 1996; Inamura *et al.*, 1997a; Moss *et al.*, 1997). In addition, voltage-gated inward and outward currents similar to those previously reported (Trotier *et al.*, 1993; Liman and Corey, 1996; Taniguchi *et al.*, 1996; Inamura *et al.*, 1997a) were observed in snake VN receptor neurons. The results described above indicate that snake VN receptor neurons have properties similar to those of other species with regard to possessing high input resistance and the voltage-gated currents that underlie the observed responses.

Snake VN neurons fired repetitively in response to small injected currents with no sign of adaptation during a  $1$  s step (Figure 2A). This observation is consistent with those in VN neurons in other species (Trotier *et al.*, 1993; Liman and Corey, 1996; Taniguchi *et al.*, 1996; Inamura *et al.*, 1997a; Moss *et al.*, 1997). Vomeronasal neurons of the frog, mouse and rat have been reported to increase their firing rates linearly with currents up to  $10$  pA (Trotier *et al.*, 1994; Liman and Corey, 1996; Inamura *et al.*, 1997a). In the snake, however, the range where firing frequency increased with an increase in the magnitude of injected currents without oscillation was narrower than that in VN neurons in other species. The snake VN neurons which fired action potentials repetitively tended to settle into oscillation in response to an injected current of  $3$ – $20$  pA. In the frog, firing of VN neurons was strongly dependent on the value of the resting membrane potential (Trotier and Døving, 1996b). For instance, long-lasting suprathreshold current pulses evoked only an initial action potential at resting membrane potential of  $-101$  mV. At more positive resting membrane voltages the cell fired repetitively in response to injected currents (Trotier and Døving, 1996a). The mean resting membrane potentials of VN neurons in snakes was more negative than those in the mouse and rat, which may be the cause of the difference in repetitive firing behavior of VN neurons as compared with those of other species.

### Response induced by IP<sub>3</sub>

The present study demonstrates that dialysis of IP<sub>3</sub> into

snake VN receptor neurons induces inward currents with an increase in membrane conductance. The current was inhibited by extracellular ruthenium red. The mean reversal potential of the IP<sub>3</sub>-induced response in snakes under the condition where the patch pipettes contained Cs<sup>+</sup>-internal solution was about  $-15$  mV, suggesting the possibility that IP<sub>3</sub>-sensitive component found in this study is evoked via cation nonspecific IP<sub>3</sub>-gated channels having a slight preference for Cs<sup>+</sup> ion. This value is less negative than those in turtle VN and rat olfactory neurons using similar K<sup>+</sup>-internal solutions (Okada *et al.*, 1994; Taniguchi *et al.*, 1995). This difference may reflect the blockage effects of internal Cs<sup>+</sup> on Ca<sup>2+</sup>-activated K<sup>+</sup> conductance which is suggested to be involved in the IP<sub>3</sub>-induced current found in turtle VN neurons and rat olfactory neurons (Okada *et al.*, 1994; Taniguchi *et al.*, 1995). As a result, the reversal potential could shift to a less negative value.

Another possible contribution to the IP<sub>3</sub>-induced response may be Cl<sup>-</sup>-conductance. We could not rule out this possibility, since the reversal potentials for nonspecific cationic channels are similar to those for Cl<sup>-</sup> channels under the experimental conditions used in this study. As seen from Figure 5, for instance, both  $I$ - $V$  relationships at base and at peak display nonlinear outward currents in the positive membrane range, although the pipette contains Cs-internal solution. This outwardly rectified component may reflect a Ca<sup>2+</sup>-activated Cl<sup>-</sup> current.

In snake VN neurons, the magnitude of the current response induced by  $100$   $\mu$ M IP<sub>3</sub> was relatively small compared with those in the turtle and the rat (Taniguchi *et al.*, 1996; Inamura *et al.*, 1997a). The voltage sensitivity of snake VN receptor neurons, however, is so high that small inward currents induced via IP<sub>3</sub>-dependent conductance can generate action potentials.

While IP<sub>3</sub> evoked an inward current in snake VN neurons dialyzed with Cs<sup>+</sup>-internal solution, the Ca<sup>2+</sup>-ionophore ionomycin or the Ca<sup>2+</sup>-ATPase inhibitor thapsigargin elicited no response under the same experimental conditions. This suggests that the IP<sub>3</sub>-induced current in the neurons is not mediated by increases in intracellular Ca<sup>2+</sup>. However, these results do not rule out the possibility that a localized increase in Ca<sup>2+</sup> is involved in chemosignal transduction (Wang *et al.*, 1997).

### Response of VN neurons to cAMP

The present study suggests that cAMP-induced conductance does not exist in snake VN neurons. Our results are consistent with those obtained from the frog, mouse and rat (Trotier *et al.*, 1993; Liman and Buck, 1994; Liman and Corey, 1996; Inamura *et al.*, 1997a), but differ from that obtained from the turtle (Taniguchi *et al.*, 1996). This discrepancy may represent a species difference. Among those animals, for instance, turtles lack a VN epithelium that is separate from a main olfactory epithelium.

We have previously demonstrated that application of



forskolin, GTP and GTP $\gamma$ S to membrane preparations of the snake VN epithelia induced cAMP accumulation (Luo *et al.*, 1994), suggesting the existence of a functional adenylyl cyclase in the snake VN sensory epithelium. We have also reported that the level of cAMP is reduced when a 20 kDa vomeronasally mediated chemoattractive protein (ES20) for garter snakes (Jiang *et al.*, 1990) binds to its G-protein-coupled receptors. Furthermore, forskolin-stimulated levels of cAMP are reduced by ES20-receptor binding. The present results, together with our prior observations, suggest the possibility that cAMP may negatively regulate a VN transduction pathway without causing a conductance change in the receptor membrane.

### IP<sub>3</sub> involvement in signal transduction for chemoattractants

Earthworm shock secretion, a known VN chemoattractant for snakes, contains a vomeronasally mediated chemoattractive protein (ES20) for garter snakes (Jiang *et al.*, 1990). Luo *et al.* (Luo *et al.*, 1994) reported that binding of ES20 to its G-protein coupled receptors increased IP<sub>3</sub> levels in membrane preparations of snake VN epithelium. The present study demonstrates that intracellular dialysis of IP<sub>3</sub> induces inward currents with an increase in membrane conductance. In addition, extracellular application of earthworm electric shock-induced secretion evokes an inward current with an average reversal potential of -21 mV (Figure 9). This value is similar to that of the response induced by IP<sub>3</sub> (Figure 5). Thus, the present study together with the previously reported observations strongly suggest that IP<sub>3</sub> acts as a second messenger in the transduction of environmental chemoattractants in the garter snake VN organ.

Involvement of an IP<sub>3</sub>-mediated pathway has also been suggested in VN transduction relating to mammalian sexual signaling. In female pigs, boar seminal fluid or urine results in a GTP-dependent increase in production of IP<sub>3</sub> (Wekesa and Anholt, 1997). A G $\alpha$ q/11-related protein was found in VN neurons, concentrated in their microvilli (Wekesa and Anholt, 1997). Patch-clamp studies on rat VN neurons have indicated that intracellular dialysis of IP<sub>3</sub> elicits a membrane conductance (Inamura *et al.*, 1997a). IP<sub>3</sub> channel blockers and phospholipase C inhibitors block the response of female rat VN neurons to urine excreted by males (Inamura *et al.*, 1997b). These observations further support the involvement of an IP<sub>3</sub>-mediated pathway in VN transduction relating to mammalian sexual signaling. Therefore it is possible that an IP<sub>3</sub>-mediated pathway is commonly utilized by vertebrates in VN transduction.

In terms of response to physiological ligands, however, differences have been reported in different species. In the mouse, a urine-derived compound, dehydroexobrevicomin elicited an outward current at a holding potential of -70 mV in 26% of VN neurons (Moss *et al.*, 1997). Application of this chemical produced membrane hyperpolarization and/or

a reduction in the firing of action potentials with a decrease in membrane conductance (Moss *et al.*, 1997). In contrast, urine excreted by male rats increased the impulse frequency in VN neurons of female rats, suggesting that male urine induced an excitatory response in this species (Inamura *et al.*, 1997b). In frogs, some VN neurons showed excitatory fluctuations in response to a brief exposure of ATP; however, ATP may not be a physiological ligand (Trotier *et al.*, 1994). In the present study chemoattractants from prey elicited an inward current with an increase in membrane conductance. It is not clear whether the direction of ligand-activated currents depends on the nature of the ligand or the species under investigation. Clearly, further study is needed to elucidate the signal transduction mechanisms underlying the response of VN receptor neurons to physiological ligands.

### Responses to chemoattractants in earthworm shock secretion

The present study has confirmed previous findings that the chemoattractants in ESS activate VN system neurons (Jiang *et al.*, 1990). In this case, we have demonstrated that these chemoattractants produce inward depolarizing currents when recorded under perforated patch-clamp conditions. It is noteworthy that we were unable to produce such responses in the conventional whole-cell configuration in any cell tested. This suggests that some soluble cellular constituent(s) are necessary for the cell's electrical response to the chemoattractant (Lucero and Papone, 1990), but not to its response to either injected second messengers or to voltage and current manipulation. These (this) soluble cellular constituent(s) may contribute to the large difference in the magnitude of the responses evoked by chemoattractant and IP<sub>3</sub>. As mentioned in the previous section, the present study and our prior biological studies strongly suggest that IP<sub>3</sub> acts as a second messenger in VN transduction in garter snakes. It is more likely that the rise in IP<sub>3</sub> levels is followed by as yet unidentified events, including a contribution of soluble cellular constituent(s) than an unknown factor other than IP<sub>3</sub> and cAMP initiating the response to the chemoattractants.

### Acknowledgements

The research was supported by NIDCD grant DC 02531 to M.H. The research reported herein was performed according to the 'Principles of Animal Care', publication no. 86-23, revised 1985 of the National Institute of Health and also to the guidelines of the Animal Care and Utilization Act, under the supervision of the SUNY Health Science Center Institutional Animal Care Committee.

### References

- Berghard, A. and Buck, L.B. (1996) *Sensory transduction in vomeronasal neurons: evidence for G $\alpha$ o, G $\alpha$ i2, and adenylyl cyclase II as major*

- components of a pheromone signaling cascade. *J. Neurosci.*, 16, 909–918.
- Berridge, M.J.** (1993) *Inositol trisphosphate and calcium signaling*. *Nature*, 361, 315–325.
- Bodian, D.A.** (1936) *A method for staining nerve fibers and nerve endings in mounted paraffin sections*. *Anat. Rec.*, 65, 89–97.
- Bodian, D.A.** (1937) *The staining of paraffin sections of nervous tissue with activated protargol: the role of fixatives*. *Anat. Rec.*, 69, 153–162.
- Dulac, C. and Axel, R.** (1995) *A novel family of genes encoding putative pheromone receptors in mammals*. *Cell*, 83, 195–206.
- Ferris, C.D. and Snyder, S.H.** (1992) *Inositol 1,4,5-trisphosphate-activated calcium channels*. *Annu. Rev. Physiol.*, 54, 469–488.
- Halpern, M.** (1987) *The organization and function of the vomeronasal system*. *Annu. Rev. Neurosci.*, 10, 325–362.
- Halpern, M., Shapiro, L.S. and Jia, C.** (1995) *Differential localization of G proteins in the opossum vomeronasal system*. *Brain Res.*, 677, 157–161.
- Hamill, O.P., Marty, A., Neher, E., Sackmann, B. and Sigworth, F.J.** (1981) *Improved patch-clamp techniques for high-resolution current recording from cells and cell-free membrane patches*. *Pflügers Arch.*, 391, 85–100.
- Herrada, G. and Dulac, C.** (1997) *A novel family of putative pheromone receptors in mammals with a topographically organized and sexually dimorphic distribution*. *Cell*, 90, 763–773.
- Inamura, K., Kashiwayanagi, M. and Kurihara, K.** (1997a) *Inositol-1,4,5-trisphosphate induces responses in receptor neurons in rat vomeronasal sensory slices*. *Chem. Senses*, 22, 93–103.
- Inamura, K., Kashiwayanagi, M. and Kurihara, K.** (1997b) *Blockage of urinary responses by inhibitors for IP<sub>3</sub>-mediated pathway in rat vomeronasal sensory neurons*. *Neurosci. Lett.*, 233, 129–132.
- Jia, C. and Halpern, M.** (1996) *Subclasses of vomeronasal receptor neurons: differential expression of G proteins (G<sub>α2</sub> and G<sub>αd</sub>) and segregated projections to the accessory olfactory bulb*. *Brain Res.*, 719, 117–128.
- Jiang, X.C., Inouchi, J., Wang, D. and Halpern, M.** (1990) *Purification and characterization of a chemoattractant from electric shock-induced earthworm secretion, its receptor binding, and signal transduction through the vomeronasal system of garter snakes*. *J. Biol. Chem.*, 265, 8736–8744.
- Liman, E.R. and Buck, L.B.** (1994) *A second subunit of the olfactory cyclic nucleotide-gated channel confers high sensitivity to cAMP*. *Neuron*, 13, 611–621.
- Liman, E.R. and Corey, D.P.** (1996) *Electrophysiological characterization of chemosensory neurons from the mouse vomeronasal organ*. *J. Neurosci.*, 16, 4625–4637.
- Liu, W., Wang, D., Chen, P. and Halpern, M.** (1997) *Cloning and expression of a gene encoding a protein obtained from earthworm secretion that is a chemoattractant for garter snakes*. *J. Biol. Chem.*, 272, 27378–27381.
- Lucero, M.T. and Papone, P.A.** (1990) *Membrane responses to nor-epinephrine in cultured brown fat cells*. *J. Gen. Physiol.*, 95, 523–544.
- Luo, Y., Lu, S., Chen, P., Wang, D. and Halpern, M.** (1994) *Identification of chemoattractant receptors and G-proteins in the vomeronasal system of garter snakes*. *J. Biol. Chem.*, 269, 16867–16877.
- Matsunami, H. and Buck, L.B.** (1997) *A multigene family encoding a diverse array of putative pheromone receptors in mammals*. *Cell*, 90, 775–784.
- Moss, R.L., Flynn, R.E., Shen, X.M., Dudley, C., Shi, J. and Novotny, M.** (1997) *Urine-derived compound evokes membrane responses in mouse vomeronasal receptor neurons*. *J. Neurophysiol.*, 77, 2856–2862.
- Okada, Y., Teeter, J.H. and Restrepo, D.** (1994) *Inositol 1,4,5-trisphosphate-gated conductance in isolated rat olfactory neurons*. *J. Neurophysiol.*, 71, 595–602.
- Okamoto, K., Tokumitsu, Y. and Kashiwayanagi, M.** (1996) *Adenylyl cyclase activity in turtle vomeronasal and olfactory epithelium*. *Biochem. Biophys. Res. Commun.*, 220, 98–101.
- Ryba, N.J. and Tirindelli, R.** (1997) *A new multigene family of putative pheromone receptors*. *Neuron*, 19, 371–379.
- Taniguchi, M., Kashiwayanagi, M. and Kurihara, K.** (1995) *Intracellular injection of inositol 1,4,5-trisphosphate increases a conductance in membranes of turtle vomeronasal receptor neurons in the slice preparation*. *Neurosci. Lett.*, 188, 5–8.
- Taniguchi, M., Kashiwayanagi, M. and Kurihara, K.** (1996) *Intracellular dialysis of cyclic nucleotides induces inward currents in turtle vomeronasal receptor neurons*. *J. Neurosci.*, 16, 1239–1246.
- Trotier, D. and Døving, K.B.** (1996a) *Direct influence of the sodium pump on the membrane potential of vomeronasal chemoreceptor neurons in frog*. *J. Physiol.*, 490, 611–621.
- Trotier, D. and Døving, K.B.** (1996b) *Functional role of receptor neurons in encoding olfactory information*. *J. Neurobiol.*, 30, 58–66.
- Trotier, D., Døving, K.B. and Rosin, J.F.** (1993) *Voltage-dependent currents in microvillar receptor cells of the frog vomeronasal organ*. *Eur. J. Neurosci.*, 5, 995–1002.
- Trotier, D., Døving, K.B. and Rosin, J.F.** (1994) *Functional properties of the vomeronasal receptor cells*. In Kurihara, K., Suzuki, N. and Ogawa, H. (eds), *Olfaction and Taste XI*. Springer-Verlag, Tokyo, pp. 188–191.
- Wang, D., Chen, P., Liu, W., Li, C.S. and Halpern, M.** (1997) *Chemosignal transduction in the vomeronasal organ of garter snakes: Ca<sup>2+</sup>-dependent regulation of adenylyl cyclase*. *Arch. Biochem. Biophys.*, 348, 96–106.
- Wang, R. and Halpern, M.** (1980) *Light and electron microscopic observations on the normal structure of the vomeronasal organ of garter snakes*. *J. Morphol.*, 164, 47–67.
- Wekesa, K.S. and Anholt, R.R.** (1997) *Pheromone regulated production of inositol-(1,4,5)-trisphosphate in the mammalian vomeronasal organ*. *Endocrinology*, 138, 3497–3504.

Accepted August 15, 1999